



Aalborg Universitet

AALBORG UNIVERSITY  
DENMARK

## Co-ordinated Control Strategy for Hybrid Wind Farms with PMSG and FSIG under Unbalanced Grid Voltage Condition

Zeng, Xin; Yao, Jun; Chen, Zhiqian; Hu, Weihao; Chen, Zhe; Zhou, Te

*Published in:*

I E E E Transactions on Sustainable Energy

*DOI (link to publication from Publisher):*

[10.1109/TSTE.2016.2527041](https://doi.org/10.1109/TSTE.2016.2527041)

*Publication date:*

2016

*Document Version*

Peer reviewed version

[Link to publication from Aalborg University](#)

*Citation for published version (APA):*

Zeng, X., Yao, J., Chen, Z., Hu, W., Chen, Z., & Zhou, T. (2016). Co-ordinated Control Strategy for Hybrid Wind Farms with PMSG and FSIG under Unbalanced Grid Voltage Condition. I E E E Transactions on Sustainable Energy, 7(3), 1100-1110. DOI: 10.1109/TSTE.2016.2527041

### General rights

Copyright and moral rights for the publications made accessible in the public portal are retained by the authors and/or other copyright owners and it is a condition of accessing publications that users recognise and abide by the legal requirements associated with these rights.

- ? Users may download and print one copy of any publication from the public portal for the purpose of private study or research.
- ? You may not further distribute the material or use it for any profit-making activity or commercial gain
- ? You may freely distribute the URL identifying the publication in the public portal ?

### Take down policy

If you believe that this document breaches copyright please contact us at [vbn@aub.aau.dk](mailto:vbn@aub.aau.dk) providing details, and we will remove access to the work immediately and investigate your claim.

# Coordinated Control Strategy for Hybrid Wind Farms with PMSG and FSIG under Unbalanced Grid Voltage Condition

Xin Zeng, Jun Yao, *Member, IEEE*, Zhiqian Chen, Weihao Hu, Zhe Chen, *Senior Member, IEEE*, and Te Zhou

**Abstract**—This paper investigates a control strategy for a wind farm with the direct-driven permanent-magnet synchronous generators (PMSG)-based wind turbines and the fixed speed induction generators (FSIG)-based wind turbines under unbalanced grid voltage condition. By controlling the PMSG-based wind farm to inject negative-sequence current for decreasing voltage unbalance factor (VUF) at point of common coupling (PCC), the double grid frequency oscillations in electromagnetic torque, active and reactive power output from the FSIG-based wind farm can be suppressed. In this paper, the maximum amplitude of the negative-sequence current provided by the PMSG-based wind farm under different average active power output and different VUF conditions is deduced, and the impacts of its phase angle on the VUF mitigation control effect are further studied. The **improved** control strategy of injecting negative-sequence current from the PMSG-based wind farm **by the modified negative-sequence voltage and current double closed-loop control system is then developed**. Finally, the correctness of theoretical analysis and the effectiveness of the proposed control strategy **are** validated by the experimental results.

**Index Terms**—Wind power generation; hybrid wind farm; unbalanced grid voltage condition; voltage unbalance factor (VUF); negative-sequence current.

## I. INTRODUCTION

With rapid development of wind power industry in recent years, a great number of wind farms have been installed all over the world. Due to the flexible power control capability, variable speed-constant frequency (VSCF) wind turbines using doubly fed induction generator (DFIG) or permanent magnetic synchronous generator (PMSG) have become dominant among the newly installed wind farms [1]. However, fixed speed wind turbines using induction generator (FSIG) still have a significant percentage in operating and under-construction wind farms because of its simple structures and lower costs [2]. The FSIG-based wind turbines are connected with the grid directly without converters, so they can't be controlled flexibly

This work is partly supported by National Natural Science Foundation of China (NSFC) (51477016).

Xin Zeng, Jun Yao (Corresponding author), Zhiqian Chen, and Te Zhou are with State Key Laboratory of Power Transmission Equipment & System Security and New Technology, School of Electrical Engineering, Chongqing University, Chongqing, 400044, China (e-mail: zxranks@sina.com; topyj@163.com; chenzhiqian@yeah.net; zhoutezone@vip.qq.com).

Weihao Hu, and Zhe Chen are with Department of Energy Technology, Aalborg University, Aalborg East DK-9220, Denmark (e-mail: whu@et.aau.dk; zch@et.aau.dk).

and can be easily affected by the grid voltage disturbance [3]-[5]. Nowadays, most wind farms are installed in rural or offshore areas where voltage unbalance condition occurs more frequently [6]-[9]. Consequently, FSIG-based wind farm directly connected to the weak grid could be seriously affected by the unbalanced grid voltage, which may even result in the disconnection of the wind farm. Due to the high negative-sequence current flowing through the stator, the overheating and losses in the generator would be obviously produced, which can destroy the insulation and decrease lifetime of the generator. Furthermore, the interaction between positive- and negative-sequence components of stator current and voltage will introduce double supply frequency oscillations in electromagnetic torque, which inevitably generates significant stress in the turbine mechanical system [10]. As a consequence, it is necessary to develop novel measures for the FSIG-based wind farm to improve its ability coping with unbalanced grid voltage condition.

At present, several control schemes **have been** investigated for improving operation performance of FSIG-based wind farm during network unbalance. In [11], a static synchronous compensator (STATCOM) equipped with FSIG-based wind farm is controlled to inject reactive power to grid for aiding grid voltage quick recover, which effectively **decreases** negative-sequence voltage at terminal of FSIG-based wind farm and **improves** ability of the wind farm riding through the voltage unbalance condition. The control effect of this scheme is significantly dependent on the capacity of the STATCOM and the line impedance between the fault location and the STATCOM. For a small VUF caused by an unbalance fault, the line impedance will have a big influence upon VUF mitigation performance, and it is difficult to determine the accurate capacity of STATCOM for achieving the satisfactory control effect [12]. Another effective scheme is using series compensation equipment such as dynamic voltage restorer (DVR) [13], which **maintains** the stator voltage balance during grid voltage unbalance. However, DVR may not endure long-time steady-state voltage unbalance fault because of its limited DC link capacity [14]. As analyzed, the two strategies stated above both effectively improve the operation performance for the FSIG-based wind farm under unbalanced grid voltage condition. However, there are still some drawbacks for both strategies, and utilizing auxiliary hardware devices will undoubtedly increase the cost of the whole system.

Recently, the distributed energy resources based PWM converters have been used to compensate the unbalanced voltage of the connected power grid during network unbalance

[15]-[17]. Obviously, the operation performance of FSIG-based wind power generation system could be improved by being installed along side these distributed energy resources. More recently, with increased installation of the **VSCF** wind turbine generation system, the hybrid wind farm combining FSIG with DFIG or PMSG-based wind farm have been a trend of large-scale wind farm construction. Therefore, the operation performance of FSIG-based wind farm could be improved by nearby DFIG or PMSG-based wind farm to cope with the requirement of grid code without auxiliary hardware devices under non-ideal grid conditions [18]-[20]. In a hybrid wind farm including FSIG-based and DFIG-based wind farm, a strategy **has been** proposed by controlling DFIG-based wind farm to inject negative-sequence current into the grid to decrease the VUF at PCC [20], which effectively **weakens** doubly supply frequency pulsations in electromagnetic torque and power output of FSIG-based wind farm. However, the amplitude of compensated negative-sequence current is limited by the rated current of the grid-side converter in the DFIG-based wind power generation system, the negative-sequence grid voltage or the VUF at PCC can't be fully compensated under some conditions such as the DFIG system working under high power generation condition. **In this case, the VUF mitigation effect by the proposed control strategy in [20] cannot be demonstrated to be optimal, which means that the available negative-sequence current cannot be adequately utilized by the control strategy in [20] for decreasing the VUF at PCC to its minimum value under some conditions. Moreover,** the VUF mitigation control effect is restricted because of the partial power converters in DFIG-based wind farm, which means that merely using the DFIG-based wind farm to compensate the voltage unbalance has limited effect on improving the operation performance for a hybrid wind farm including FSIG-based and DFIG-based wind farm during network unbalance. Compared with the DFIG-based wind power generation system, the PMSG-based wind turbine uses full scale converters to transmit wind power to the power grid, as a result, hybrid wind farms containing PMSG-based and FSIG-based wind power generation systems may have more flexible controllability to mitigate the unbalanced voltage at PCC without utilizing any other hardware devices such as STATCOM or DVR, whereas there has been a little work on this topology. In order to illustrate the effectiveness of a compensation control strategy, the statement "optimal value of VUF at PCC" **is** introduced in this paper. Due to the limited amplitude of current provided by the PMSG-based wind farm, the VUF at PCC will be controlled to various values with different average active power outputs of PMSG-based wind farms. However, there always exists a lowest level VUF at PCC with a given average active power output of PMSG-based wind farm, which can minimize the double grid frequency oscillations in electromagnetic torque, active and reactive power output from the FSIG-based wind farm. The lowest level VUF at PCC can be defined as the optimal value of VUF at PCC.

In this paper, a hybrid wind farm which consists of FSIG-based wind farm and PMSG-based wind farm is chosen as the studied case. The maximum amplitude of negative-sequence current generated by the PMSG-based wind

farm is firstly deduced, and then the effect of phase angle of the negative-sequence current with different VUF at terminal of PMSG-based wind farm is analyzed, which can be used for demonstrating the control effect of the proposed control strategy. Based on the theoretical analysis, a coordinated control strategy for decreasing VUF at PCC by using PMSG-based wind farm is developed to enhance the operation performance of the FSIG-based wind farm. Although the control strategy of unbalanced voltage compensation by injecting negative-sequence current has been **studied preliminary** in other papers, the influence caused by the phase angle of the negative-sequence current has not been investigated. **In addition, the existed control strategy cannot achieve the optimal control effect for the unbalanced voltage compensation under some conditions, especially when the negative-sequence voltage cannot be suppressed to zero within the maximum negative-sequence current amplitude. In this paper, one of the novel contributions of this paper is the depth theoretical analysis about the impact of the injected negative-sequence current phase angle to VUF at terminal of wind farm. Based on the theoretical analysis, the improved unbalanced voltage compensation control strategy is proposed by designing a new negative-sequence voltage and current double closed-loop control system, and it can be generally utilized for improving the operation performance of hybrid energy system based on full-scale PWM converter, i.e. induction generators with full scale converters or photovoltaic power system, more than PMSG-based wind power generation system during network unbalance, which is the other novel contribution of this paper.**

The paper is structured as follows. Topology and mathematical model of the investigated system is introduced in section II. Section III deduces the maximum amplitude of negative-sequence current output of PMSG-based wind farm under different operation conditions. Section IV proposes a control strategy to decrease the VUF at PCC to its optimal value. Verification about the proposed control strategy is demonstrated by using experimental results in section V, and section VI draws the conclusion.

## II. TOPOLOGY AND MODEL OF THE HYBRID WIND FARM

### A. Topology of the hybrid wind farm

Configuration of the hybrid wind farm including PMSG-based wind farm of 30MW rated capacity and FSIG-based wind farm of 20MW rated capacity is shown in Fig. 1.

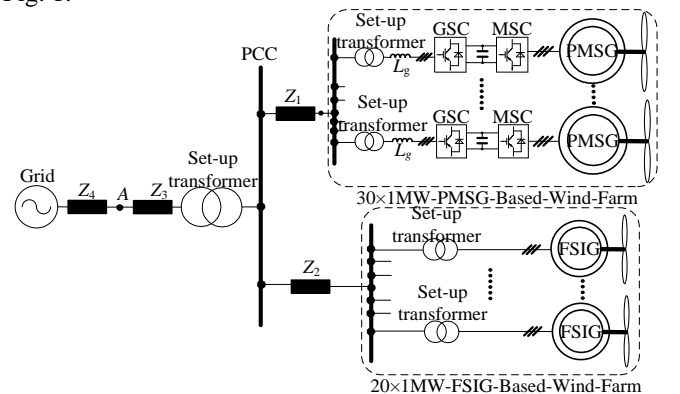


Fig. 1 Configuration of a grid-connected hybrid wind farm.

Although the given proportion of the two wind farms does not represent a real installation, there are a number of existing wind farms which have both PMSG and FSIG in the range of around tens MW. The PMSG-based wind farm consists of 30 1MW PMSG-based wind turbines, and the FSIG-based wind farm consists of 20 1MW FSIG-based wind turbines. The 30MW PMSG-based wind farm and 20MW FSIG-based wind farm can be equivalent to a PMSG-based wind turbine of 30MW rated capacity and a FSIG-based wind turbine of 20MW rated capacity respectively without considering the effect among wind power generators in wind farms.  $Z_1$ ,  $Z_2$ ,  $Z_3$  and  $Z_4$  are impedance of the transmission lines respectively.

### B. Model of the hybrid wind farm during network unbalance

Operation principles and mathematical models under normal operation conditions about PMSG-based wind farm and FSIG-based wind farm have been developed in details in [1] and [21] respectively, so a brief description is given here.

Under unbalanced grid voltage condition, machine-side converter (MSC) of PMSG-based wind power generation systems can still be controlled to obtain steady DC link voltage as normal. However, control of grid-side converter (GSC) of PMSG systems may be modified for improving the unbalanced operation capability for the FSIG-based wind farm. Mathematical model of GSC in the positive/negative sequence synchronous reference frames can be expressed as

$$\begin{cases} V_{gd+}^+ = -R_g i_{gd+}^+ + \omega_1 L_g i_{gq+}^+ + U_{gd+}^+ - L_g \frac{di_{gd+}^+}{dt} \\ V_{gq+}^+ = -R_g i_{gq+}^+ - \omega_1 L_g i_{gd+}^+ + U_{gq+}^+ - L_g \frac{di_{gq+}^+}{dt} \end{cases} \quad (1)$$

$$\begin{cases} V_{gd-}^- = -R_g i_{gd-}^- - \omega_1 L_g i_{gq-}^- + U_{gd-}^- - L_g \frac{di_{gd-}^-}{dt} \\ V_{gq-}^- = -R_g i_{gq-}^- + \omega_1 L_g i_{gd-}^- + U_{gq-}^- - L_g \frac{di_{gq-}^-}{dt} \end{cases} \quad (2)$$

where  $U_g$  is voltage at terminal of PMSG-based wind farm;  $V_g$  is voltage on AC side of GSC;  $i_g$  is current of GSC;  $L_g$  is total inductance including leakage inductance of transformer and line inductance;  $R_g$  is the line resistor;  $\omega_1$  is synchronous rotating angular speed; subscript  $d$  and  $q$  express components in  $d$  and  $q$  axes respectively; subscripts  $+$  and  $-$  express positive- and negative-sequence components respectively, and superscripts  $+$  and  $-$  express positive- and negative-sequence synchronous rotating reference frames respectively.

Under unbalanced grid voltage condition, average active power output ( $P_{g-av}$ ) and reactive power output ( $Q_{g-av}$ ) of PMSG-based wind farm are determined by both positive- and negative-sequence components of voltage and current [22], and they can be expressed as

$$\begin{cases} P_{g-av} = \frac{3}{2} (U_{gd+}^+ i_{gd+}^+ + U_{gq+}^+ i_{gq+}^+ + U_{gd-}^- i_{gd-}^- + U_{gq-}^- i_{gq-}^-) \\ Q_{g-av} = \frac{3}{2} (U_{gd+}^+ i_{gq+}^+ - U_{gq+}^+ i_{gd+}^+ + U_{gd-}^- i_{gq-}^- - U_{gq-}^- i_{gd-}^-) \end{cases} \quad (3)$$

## III. NEGATIVE-SEQUENCE CURRENT OF PMSG-BASED WIND FARM

### A. Negative-sequence Current Limit Analysis

Under unbalanced grid voltage condition, control for average active power output of PMSG-based wind farm should be the same with that under normal condition. Considering that the positive-sequence component of grid voltage changes quite small under unbalanced grid condition comparing with that under grid faults, there is no need to inject reactive power into the network for supporting the power grid [23]-[24]. Therefore, it is unnecessary for wind farm to inject reactive power into the network for supporting the positive-sequence voltage. Consequently, according to (1), (2) and (3), negative-sequence current output of PMSG-based wind farm is limited by considering the average active power output of PMSG systems and DC link voltage. **When the zero-sequence current component is reasonably ignored**, the limiting conditions can be expressed as

$$I_{gm-} \leq I_{gm} - \frac{P_{g-av}}{|U_{g+}^+|}; \quad I_{gm-} \leq \frac{k_m V_{dc} - |U_{g+}^+| - |U_{g-}^-|}{\omega_1 L_g} \quad (4)$$

Where  $I_{gm-}$  is amplitude of negative-sequence current;  $I_{gm}$  is the rated current of GSC;  $|i_{g+}^+|$  is amplitude of positive-sequence current determined by the average active and reactive power output of PMSG-based wind farm;  $k_m$  is the modification factor;  $|U_{g+}^+|$  and  $|U_{g-}^-|$  are amplitudes of positive- and negative-sequence voltages at terminal of PMSG-based wind farm, and  $V_{dc}$  is DC link voltage.

To deduce the negative-sequence current limit, the base values of the PMSG-based wind farm are listed in Tab. 1.

Parameters	Base values	Parameters	Base values
Voltage (V)	563	Current (kA)	35.524
Capacity (MVA)	30	Impedance ( $\Omega$ )	0.0158
DC link	1200	Modulation	$1/\sqrt{3}$
Voltage(V)		Factor	

During network unbalance, the amplitude of positive-sequence voltage is assumed to be 1.0 p.u. for simplifying the following analysis [20]. Under this scenario, the amplitude of negative-sequence current limited by average active power output and DC link voltage of PMSG systems can be further expressed as

$$\begin{aligned} I_{gm-} &\leq I_{gm} - |i_{g+}^+| = 1.05 - P_{g-av} \\ I_{gm-} &\leq \frac{k_m V_{dc} - |U_{g+}^+| - |U_{g-}^-|}{\omega_1 L_g} = 1.163 - \frac{\delta}{0.1982} \end{aligned} \quad (5)$$

Where  $\delta = |U_{g-}^-|/|U_{g+}^+|$  is voltage unbalance factor (VUF) at terminal of PMSG-based wind farm.  $L_g$  is equal to 0.1982 p.u. and  $\omega_1$  is equal to 1.0 p.u.

According to the analysis mentioned above, the amplitude of negative-sequence current generated by the PMSG-based wind farm with different VUF ( $\delta$ ) and average active power output ( $P_{g-av}$ ) is shown in Fig. 2. It can be seen that if average active power output of PMSG-based wind farm is at low value region, the maximum amplitude of negative-sequence current is primarily limited by the DC link voltage, and with the VUF increasing, the negative-sequence current limit would decrease. On the other hand, if the average active power output is at a higher value region, the amplitude of positive-sequence current flowing through GSC is high correspondingly, so the

negative-sequence current is primarily limited by the average active power output of the PMSG systems. Also, the maximum amplitude of negative-sequence current injected to the grid would decrease when the output average active power increases. As a result, the available negative-sequence current region can be determined by comprehensively considering limitation of the current rating and DC link voltage.

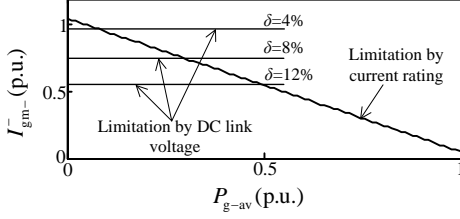


Fig. 2 Negative-sequence current limit of PMSG-based wind farm with different VUF and average active power output.

### B. Negative-sequence Current Phase Angle Analysis

Under unbalanced grid voltage condition, the phase angle of negative-sequence current also has influence on control effect for decreasing VUF at PCC. When PMSG-based wind farm is controlled to output negative-sequence current, the equivalent negative-sequence network of the studied system can be shown in Fig. 3.  $U_{D-}$  is the equivalent negative-sequence voltage source of the network, and  $i_{g-}$  is the equivalent negative-sequence current source of PMSG-based wind farm.  $Z_{FSIG}$  and  $Z_{PMSG}$  are equivalent negative-sequence impedance of FSIG-based wind farm and PMSG-based wind farm respectively.

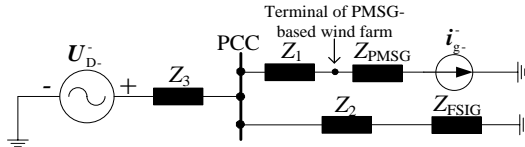


Fig. 3 Negative-sequence network with negative-sequence current output of PMSG-based wind farm.

From Fig. 3, the negative-sequence voltage at PCC ( $U_{p-}$ ) can be expressed as

$$U_{p-} = U_{D-} \cdot \frac{Z_3 // (Z_2 + Z_{FSIG})}{Z_3} - i_{g-} \cdot (Z_3 // (Z_2 + Z_{FSIG})) \quad (6)$$

By using  $\beta = (Z_3 // (Z_2 + Z_{FSIG})) / Z_3$ ,  $Z_5 = Z_3 // (Z_2 + Z_{FSIG})$ , (6) can be simplified as:

$$U_{p-} = \beta U_{D-} - i_{g-} \cdot Z_5 \quad (7)$$

From (6) and (7), the minimum amplitude of negative-sequence voltage at PCC will be obtained when  $-i_{g-} \cdot Z_5$  and  $\beta U_{D-}$  are phase-reversed. The amplitude and phase angle of the equivalent negative-sequence voltage source  $U_{D-}$  may change when different grid voltage condition occurs, which means that the phase angle of negative-sequence current vector that is needed to compensate the negative-sequence voltage should be dependent on the grid voltage unbalance condition. If the phase angle of the compensation current is not proper, the increment of the amplitude of negative-sequence voltage at PCC may be resulted in.

As can be seen from Fig. 3, the negative-sequence voltage at terminal of PMSG-based wind farm ( $U_{g-}$ ) can be expressed as

$$\begin{aligned} U_{g-} &= U_{p-} - i_{g-} \cdot Z_1 \\ &= \beta U_{D-} - i_{g-} \cdot (Z_1 + Z_5) \end{aligned} \quad (8)$$

The amplitude of negative-sequence voltage at terminal of PMSG-based wind farm ( $U_{g-}$ ) can be obtained as

$$|U_{g-}| = \sqrt{|\beta U_{D-}|^2 + |-i_{g-} \cdot Z_6|^2 + 2|\beta U_{D-}| \cdot |-i_{g-} \cdot Z_6| \cdot \cos \theta} \quad (9)$$

Where  $Z_6 = Z_1 + Z_5$ , and  $\theta$  is angle between  $-i_{g-} \cdot Z_6$  and  $\beta U_{D-}$ .

Considering  $\beta$  and  $Z_6$  are constant during the network unbalance, the angle  $\theta$  between  $-i_{g-} \cdot Z_6$  and  $\beta U_{D-}$  is only related to the phase angle of negative-sequence current, which means that the impact of angle  $\theta$  on the amplitude of negative-sequence voltage at PCC is the same with the phase angle of  $i_{g-}$ . Taking into account the fact that the transmission lines between the wind farm and PCC are usually very short and the impedance of FSIG are very small, according to (8) and (9), the negative-sequence voltage at PCC is similar to that at terminal of PMSG-based wind farm by neglecting impedance  $Z_1$  and  $Z_5$ . As a result, the optimal VUF at PCC can be achieved by controlling the negative-sequence voltage at terminal of PMSG-based wind farm to a minimum value. Fig. 4 shows the trajectories of the negative-sequence voltage vectors and curves of relationship between the amplitude of negative-sequence voltage vector at terminal of PMSG-based wind farm and angle  $\theta$ .

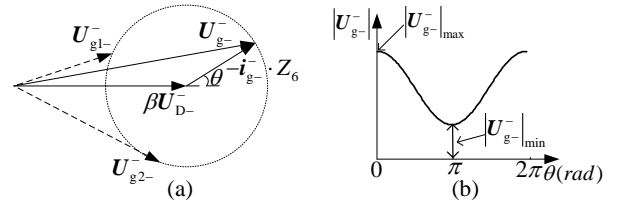


Fig. 4 (a) Trajectories of negative-sequence voltage vectors; (b) Amplitude of negative-sequence voltage versus angle  $\theta$ .

As can be seen from Fig. 4, the amplitude of negative-sequence voltage vector at terminal of PMSG-based wind farm ( $|U_{g-}|$ ) will vary as cosine law periodically when angle  $\theta$  varies from 0 to  $2\pi$ . As the maximum negative-sequence current generated by the PMSG systems is limited by the rated current of the GSC and the DC link voltage, when the negative-sequence voltage generated by the power grid ( $U_{D-}$ ) is at a high value, the negative-sequence voltage at terminal of PMSG-based wind farm ( $U_{g-}$ ) can't be decreased to zero no matter what the phase angle of negative-sequence current is. In addition, the phase angle of negative-sequence current has a big impact on control effect for voltage unbalance, and under a certain condition, there exists an optimal value for minimizing the VUF, as shown in Fig. 4 (b). As a consequence, the amplitude and phase angle of the compensated negative-sequence current will significantly affect the VUF mitigation control effect during network unbalance. In order to improve the operation performance of the associated FSIG-based wind farm under unbalanced grid voltage condition, the amplitude and phase angle of negative-sequence current output of PMSG-based wind farm should be considered synthetically for decreasing VUF at PCC.

#### IV. CONTROL STRATEGY OF THE HYBRID WIND FARM DURING NETWORK UNBALANCE

##### A. PMSG Control for Unbalanced Voltage Compensation

Under unbalanced grid voltage condition, MSCs of PMSG systems are controlled to obtain steady DC link voltage as that under normal condition. Positive-sequence components of voltage and current of GSC are used to control output average active power of PMSG-based wind farm, which means that the positive-sequence current of GSC is controlled as that under normal condition as mentioned in [25]-[27].

It can be known from the above analysis, the VUF mitigation effect is depended on the amplitude and phase angle of the compensated negative-sequence current of PMSG system. The amplitude must be below the limitation by considering average active power output and DC link voltage, and the phase angle should be obtained with appropriate scheme.

For the negative-sequence system, the relationship between  $-i_{\text{g}}^- \cdot Z_6$  and  $U_{\text{g}}^-$  can be expressed as

$$U_{\text{g}}^- = -i_{\text{g}}^- \cdot Z_6 + \Delta U_{\text{g}}^-, \quad \Delta U_{\text{g}}^- = \beta U_{\text{D}}^- \quad (10)$$

In the negative-sequence synchronous rotating reference frame, the dq model can be expressed as

$$\begin{cases} U_{\text{gd}}^- = -i_{\text{gd}}^- \cdot R_6 + i_{\text{gq}}^- \cdot X_6 + \Delta U_{\text{gd}}^- \\ U_{\text{gq}}^- = -i_{\text{gq}}^- \cdot R_6 - i_{\text{gd}}^- \cdot X_6 + \Delta U_{\text{gq}}^- \end{cases} \quad (11)$$

where  $R_6$  and  $X_6$  are resistance and reactance of  $Z_6$  respectively.

By ignoring  $R_6$ , (11) can be simplified as

$$\begin{cases} U_{\text{gd}}^- = i_{\text{gq}}^- \cdot X_6 + \Delta U_{\text{gd}}^- \\ U_{\text{gq}}^- = -i_{\text{gd}}^- \cdot X_6 + \Delta U_{\text{gq}}^- \end{cases} \quad (12)$$

As a result, the required negative-sequence current of PMSG system can be expressed as

$$\begin{cases} i_{\text{gq}}^- = (U_{\text{gd}}^- - \Delta U_{\text{gd}}^-) / X_6 \\ i_{\text{gd}}^- = (\Delta U_{\text{gq}}^- - U_{\text{gq}}^-) / X_6 \end{cases} \quad (13)$$

From (13), if the voltage unbalance factor and the output active power are both at lower values, the required negative-sequence currents  $i_{\text{gq}}^-$  and  $i_{\text{gd}}^-$  of GSC could be generated to fully compensate the negative-sequence voltage at the terminal of the PMSG-based wind farm, and they can be expressed as

$$\begin{cases} i_{\text{gq}}^- = -\Delta U_{\text{gd}}^- / X_6 \\ i_{\text{gd}}^- = \Delta U_{\text{gq}}^- / X_6 \end{cases} \quad (14)$$

However, if the VUF at PCC is high or the PMSG systems work at high power generation condition, the negative-sequence voltage at the terminal of PMSG-based wind farm cannot be controlled to zero, which demonstrates the aforementioned theoretical analysis. In addition, because of the unknown parameters of the transmission lines, the accurate negative-sequence current reference could not be achieved in such a case. To solve this problem, an improved negative-sequence voltage and current double closed-loop control scheme is designed in this paper.

If the negative-sequence voltage at terminal of PMSG-based wind farm can be controlled to zero within the limitation of the negative-sequence current, the optimal negative-sequence current phase angle and the corresponding references can be obtained by the outer negative-sequence voltage control loops, which is defined as Mode 1.

The regulation values generated by the PI controllers in negative-sequence voltage control loops are the required negative-sequence current  $I_{\text{gq}}^{*-}$  and  $I_{\text{gd}}^{*-}$  to fully compensate the negative-sequence voltage, which can be expressed as

$$\begin{cases} I_{\text{gq}}^{*-} = [K_p(\tau_i s + 1) / \tau_i s](0 - U_{\text{gd}}^-) \\ I_{\text{gd}}^{*-} = -[K_p(\tau_i s + 1) / \tau_i s](0 - U_{\text{gq}}^-) \end{cases} \quad (15)$$

Where  $K_p$  and  $\tau_i$  are proportional coefficient and integral time constant of PI controllers in the negative-sequence voltage control loop respectively.

However, when the VUF at PCC is high or the PMSG systems work at high power generation condition, the negative-sequence voltage at terminal of PMSG-based wind farm cannot be fully compensated. In this case, one or both of the PI controller regulation values in the negative-sequence voltage control loops will be limited by the controller limitation, which indicates that the optimal negative-sequence current phase angle cannot be obtained by outer negative-sequence voltage control loops. As a consequence, an improved control strategy is investigated in this paper to obtain the optimal phase angle  $\theta_{\text{opt}}$  and the corresponding references for achieving the optimal VUF at PCC under such condition.

As can be seen from Fig.3, when zero negative-sequence current is injected, the negative-sequence voltage at terminal of PMSG-based wind farm is defined as  $U_{\text{g}0}^-$ , and it can be expressed as

$$U_{\text{g}0}^- = U_{\text{D}}^- \cdot \frac{Z_3 / (Z_2 + Z_{\text{FSIG}})}{Z_3} = \beta U_{\text{D}}^- \quad (16)$$

From (16),  $U_{\text{g}0}^-$  and  $U_{\text{D}}^-$  are in the same phase when all line resistors are ignored. As a result, the phase angle of  $U_{\text{D}}^-$  can be expressed as

$$\alpha = \arctan(U_{\text{Dq}}^- / U_{\text{Dd}}^-) = \arctan(U_{\text{gq}0}^- / U_{\text{gd}0}^-) \quad (17)$$

where  $\alpha$  is the phase angle of  $U_{\text{D}}^-$ , related to  $d$  axis of the negative-sequence synchronous rotating reference frame.

As shown in Fig. 4, when the amplitude of negative-sequence voltage at terminal of PMSG-based wind farm ( $|U_{\text{g}}^-|$ ) reaches its minimum value, the term  $-i_{\text{g}}^- \cdot Z_6$  is phase-reversed with the voltage vector  $U_{\text{g}}^-$ . In other words, the optimal VUF at PCC can be achieved if  $i_{\text{g}}^- \cdot Z_6$  and  $U_{\text{D}}^-$  are in the same phase, and the negative-sequence current phase angle is the optimal phase angle, which can be expressed as

$$\theta_{\text{opt}} = \arctan(i_{\text{gq}}^- / i_{\text{gd}}^-) = \alpha - \frac{\pi}{2} \quad (18)$$

where  $\theta_{\text{opt}}$  is the optimal negative-sequence current phase angle, related to the  $d$  axis of the negative-sequence synchronous rotating reference frame.

Based on the calculated phase angle  $\theta_{\text{opt}}$ , the negative-sequence current references can be obtained by (19) for achieving the optimal VUF at PCC. As analyzed above, the optimal negative-sequence current phase angle  $\theta_{\text{opt}}$  and corresponding references can be obtained according to

Equation (16)-(19) and the sampled negative-sequence voltage  $U_{g0}^-$  before negative-sequence current being injected under such condition, which is defined as Mode 2.

$$\begin{cases} I_{gd-}^{*-} = I_{gm-}^- \cdot \cos \theta_{opt} \\ I_{gq-}^{*-} = I_{gm-}^- \cdot \sin \theta_{opt} \end{cases} \quad (19)$$

For the inner negative-sequence current control loop, according to (2), the dq-axis control voltages in the negative-sequence rotating reference frames can be deduced as

$$\begin{cases} V_{gd-}^- = [K_{PI}(\tau_{il}s + 1)/\tau_{il}s](I_{gd-}^{*-} - i_{gd-}^-) - \omega_1 L_g i_{gq-}^- + U_{gd-}^- \\ \quad = [K_{PI}(\tau_{il}s + 1)/\tau_{il}s](I_{gd-}^{*-} - i_{gd-}^-) + \Delta V_{gd-}^- \\ V_{gq-}^- = [K_{PI}(\tau_{il}s + 1)/\tau_{il}s](I_{gq-}^{*-} - i_{gq-}^-) + \omega_1 L_g i_{gd-}^- + U_{gq-}^- \\ \quad = [K_{PI}(\tau_{il}s + 1)/\tau_{il}s](I_{gq-}^{*-} - i_{gq-}^-) + \Delta V_{gq-}^- \end{cases} \quad (20)$$

Where  $K_{PI}$  and  $\tau_{il}$  are proportional coefficient and integral time constant of PI controllers in the negative-sequence current

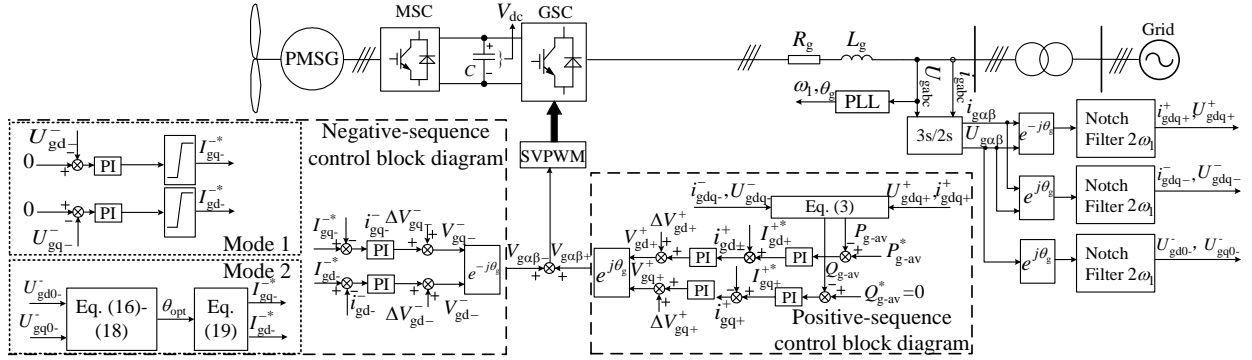


Fig. 5 Control block diagram of GSC in PMSG-based wind farm under unbalanced grid voltage condition.

### B. Impact of Transmission Network Impedance

As the PMSG system is controlled to reduce its terminal voltage unbalance, according to (10), the respective expressions can be obtained as

$$\begin{cases} i_{gq-}^- = \frac{L_2 + L_3 + L_{FSIG}}{L_1(L_2 + L_3 + L_{FSIG}) + L_3(L_2 + L_{FSIG})} U_{gd-}^- \\ \quad - \frac{L_2 + L_{FSIG}}{L_1(L_2 + L_3 + L_{FSIG}) + L_3(L_2 + L_{FSIG})} U_{Dd-}^- \\ i_{gd-}^- = -\frac{L_2 + L_3 + L_{FSIG}}{L_1(L_2 + L_3 + L_{FSIG}) + L_3(L_2 + L_{FSIG})} U_{gq-}^- \\ \quad + \frac{L_2 + L_{FSIG}}{L_1(L_2 + L_3 + L_{FSIG}) + L_3(L_2 + L_{FSIG})} U_{Dq-}^- \end{cases} \quad (21)$$

where all the line resistor values are ignored, and  $L_1$ ,  $L_2$ ,  $L_3$ , and  $L_{FSIG}$  are inductances of  $Z_1$ ,  $Z_2$ ,  $Z_3$  and  $Z_{FSIG}$  respectively.

Assuming the negative-sequence voltage at terminal of PMSG-based wind farm can be decreased to zero, the required  $d$ -axis and  $q$ -axis negative-sequence current amplitudes can be expressed as

$$\begin{cases} |i_{gq-}^-| = \frac{1}{\frac{L_1}{L_2 + L_{FSIG}} + \frac{L_1 L_3}{L_2 + L_{FSIG}} + L_3} |U_{Dd-}^-| \\ |i_{gd-}^-| = \frac{1}{\frac{L_1}{L_2 + L_{FSIG}} + \frac{L_1 L_3}{L_2 + L_{FSIG}} + L_3} |U_{Dq-}^-| \end{cases} \quad (22)$$

control loop respectively, and  $\Delta V_{gd-}^-$  &  $\Delta V_{gq-}^-$  are compensating voltages of  $d$  and  $q$  axes for decoupling control respectively.

The overall control block diagram of GSC in PMSG system during network unbalance is shown in Fig. 5. If the negative-sequence voltage at terminal of PMSG-based wind farm can be fully suppressed within the limitation, the reference values of the negative-sequence current should be calculated with Mode 1 for achieving the optimal VUF at PCC (the optimal value is zero under this condition). On the other hand, once one or both of the PI controller regulation values in the negative-sequence voltage control loop is limited by the controller limitation, Mode 2 should be adopted to calculate the negative-sequence current references for achieving the optimal VUF at PCC.

From (22), the required negative-sequence current for fully compensating the unbalanced voltage at the PMSG terminal is affected by the impedances of the transmission network. Equation (22) indicates that  $L_1$  and  $L_3$  have a positive effect, whereas  $L_2$  and  $L_{FSIG}$  have a negative effect on the reduction of voltage unbalance at the PMSG terminal. In other words, the further the PMSG-based farm is located to the fault location, the lower required negative-sequence current, and the more significant the control will be on negative-sequence voltage compensation at the PMSG terminal. In addition, the smaller the negative-sequence impedance of FSIG system, the lower required negative-sequence current, the better the unbalance voltage compensation at the PMSG terminal.

## V. EXPERIMENTAL STUDIES

As analyzed in Section II, hybrid wind farms with FSIG and PMSG can be equivalent to a wind power system combining a PMSG-based wind turbine and a FSIG-based wind turbine with the corresponding rated capacities respectively. Consequently, the experimental hybrid generators-based wind power system made up by a PMSG and a FSIG is conducted for verifying the correctness of the theoretical analysis and effectiveness of the proposed control scheme. The schematic diagram and the setup of the experimental system are shown in Fig. 6 and Fig. 7 respectively, and the detailed parameters of the test system are given in Appendix A.

As shown in Fig. 6 and Fig. 7, PMSG and FSIG are driven by an induction motor and a DC motor respectively, and the grid voltage unbalance is generated by using a voltage divider made of series and parallel inductors. In addition, due to the short transmission lines between PCC and the wind power system can be neglected, the PCC voltage is equal to the terminal voltage of PMSG in the experimental system. Therefore, the PCC voltage can be controlled directly by PMSG under grid voltage unbalance condition. During the experiment, the whole system works under a small grid voltage unbalance condition, and the VUF at PCC is about 3%. The average output active power of FSIG system is set at 2.4 kW (0.45 p.u.), and the DC link voltage of the PMSG system is controlled at 650 V.

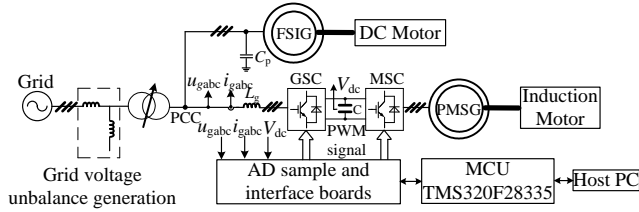


Fig.6 Schematic diagram of the experimental system.

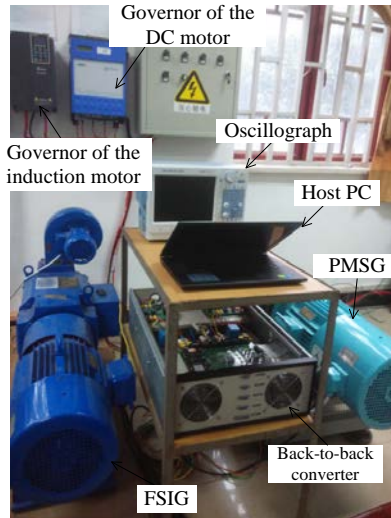


Fig.7 Experimental setup in the lab.

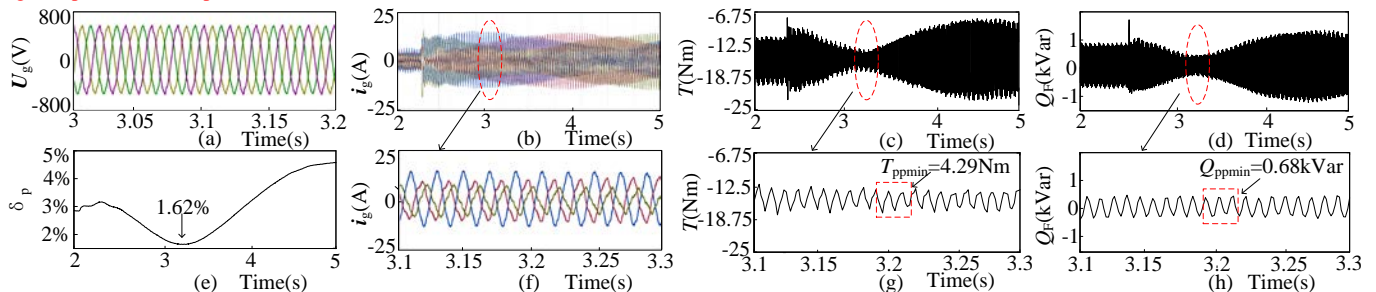


Fig.8 Experimental results by varying phase angle of negative-sequence current with 0.36 p.u. average active power output of PMSG system.

In order to verify the theoretical analysis in Section III, the experimental work by varying negative-sequence current phase angle from 0 to  $2\pi$  with 0.36 p.u. average active power output of PMSG system is carried out, and the measured waveforms are shown in Fig. 8. As seen from Fig. 8(e), Fig. 8(c) and (g), Fig. 8(d) and (h), when the phase angle of the negative-sequence current injected to the grid varies from 0 to  $2\pi$ , the VUF at PCC ( $\delta_p$ ) and the peak-to-peak pulsation values of the electromagnetic torque and reactive power output of FSIG system ( $T$  and  $Q_F$ ) vary as cosine law, which demonstrates the analysis mentioned in Section III. Meanwhile, there exists an optimal phase angle to make the VUF at PCC ( $\delta_p$ ) drop to the minimum value, which also leads to the peak-to-peak pulsation values of the electromagnetic torque and reactive power output of FSIG system ( $T$  and  $Q_F$ ) to the optimal values. In addition, it can be seen from (f) of Fig. 8, the output current of PMSG system ( $i_g$ ) is asymmetric because of the negative-sequence current generated by the GSC.

To verify the effectiveness of the proposed control scheme, experiment is conducted with the proposed control scheme with 0.36 p.u. average active power output of PMSG system, as shown in Fig. 9. As can be seen from Fig. 9(e), with the proposed control strategy, the VUF at PCC ( $\delta_p$ ) is drop to 1.62%, which is corresponding with the optimal value shown in Fig. 8(e). Compared with Fig. 8(g) and (h), Fig. 9(g) and (h) also show that the peak-to-peak double supply frequency oscillations in the electromagnetic torque and output reactive power of FSIG-based wind farm ( $T$  and  $Q_F$ ) can be decreased to optimal values, which means that the proposed control strategy effectively mitigates the VUF at PCC ( $\delta_p$ ) and improves the operation performance for the FSIG system.



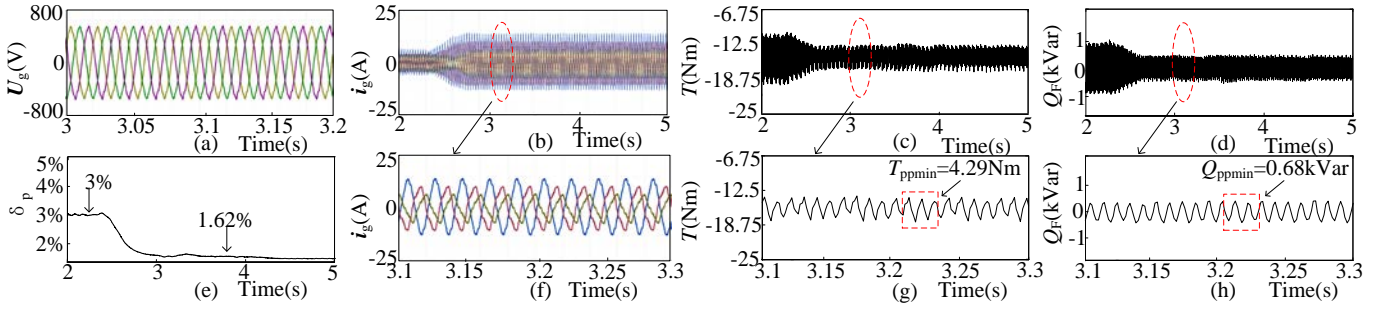


Fig.9 Experimental results with proposed control strategy with 0.36 p.u. average active power output of PMSG system.

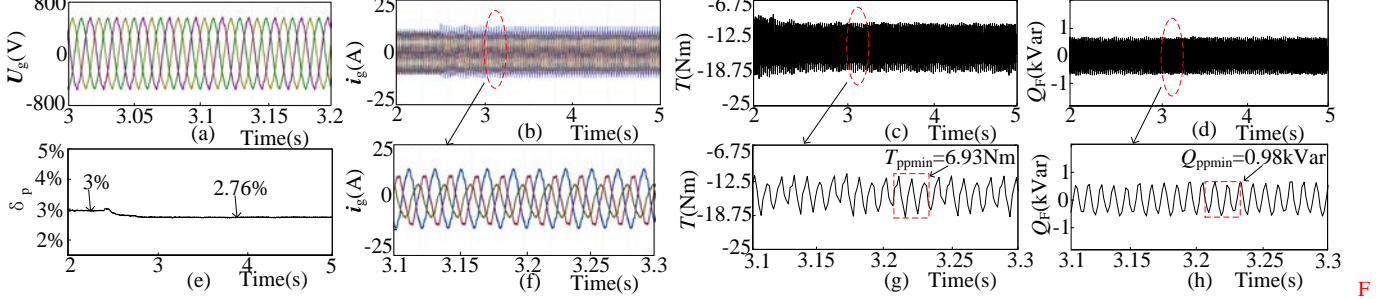


Fig.10 Experimental results with proposed control strategy with 0.88p.u. average active power output of PMSG system.

For contrast, experiment of the hybrid generators is further done at 0.88p.u. average active power output of PMSG-based wind farm with 3% VUF at PCC, as shown in Fig. 10. Due to the maximum amplitude of negative-sequence current ( $i_{g-}$ ) is mainly limited by the average active power output under such condition, which leads to higher VUF at PCC ( $\delta_p$ ), as shown in Fig. 10(e). Accordingly, the double supply frequency oscillations in electromagnetic torque and reactive power output of FSIG-based wind farm ( $T$  and  $Q_f$ ) cannot be drop to the degree compared with those in Fig. 9.

Experimental results shown above demonstrate that the proposed control strategy can control VUF at PCC to the optimal value, which effectively decreases the peak-to-peak double supply frequency pulsations in electromagnetic torque and reactive power output of FSIG system. As a consequence, the operation performance of FSIG system can be effectively improved by utilizing the proposed control strategy during network unbalance.

To further illustrate the robustness of the proposed control strategy, the system response with both a step change of average active power output and VUF at PCC are carried out. Fig. 11 shows the experimental results when a step change of PMSGs' average active power output from 0.88 p.u. to 0.36 p.u. at 4s with 3% VUF at PCC. As shown in Fig. 11(e), when the output average active power of PMSG steps during the operation process of the experimental system, VUF at PCC ( $\delta_p$ ) can be controlled to 2.76% and 1.59% with a step change of

active power respectively, which are the optimal values compared with those in (e) of Fig. 9 and Fig. 10. The VUF at PCC ( $\delta_p$ ) and the peak-to-peak pulsation values in electromagnetic torque and reactive power output of FSIG-based wind turbine ( $T$  and  $Q_f$ ) can also be controlled to the optimal values simultaneously, as can be seen by comparing Fig. 11(g) and (h) with those in Fig. 9 and Fig. 10.

Experiments with variable VUF at PCC at 0.88 p.u. average active power output of the PMSG system with the proposed control strategy are shown in Fig. 12. During the whole operation process, the VUF at PCC is changed from 3% to 0.6% at 4s, and the PMSG system is controlled to mitigate the VUF at PCC with the proposed control strategy. It is obvious that the operation performances of the hybrid wind power generation system with the variation of VUF at PCC are nicely demonstrated. With the proposed control strategy, as can be seen in Fig. 12(e), the VUF at PCC ( $\delta_p$ ) can be controlled to 2.76% and 0.49%, which are the optimal values compared with that in Fig. 10(e). At the same time, as shown in Fig. 12(g) and (h), the peak-to-peak pulsation values in the electromagnetic torque and reactive power output of FSIG system ( $T$  and  $Q_f$ ) can also be decreased to the minimum values, as compared with those in Fig. 10(g) and (h). From Fig. 11 and Fig. 12, it can be concluded that the proposed control strategy achieves the satisfactory dynamic and robust performance, which is greatly benefit for improving operation performance of FSIG system under unbalanced grid voltage condition.

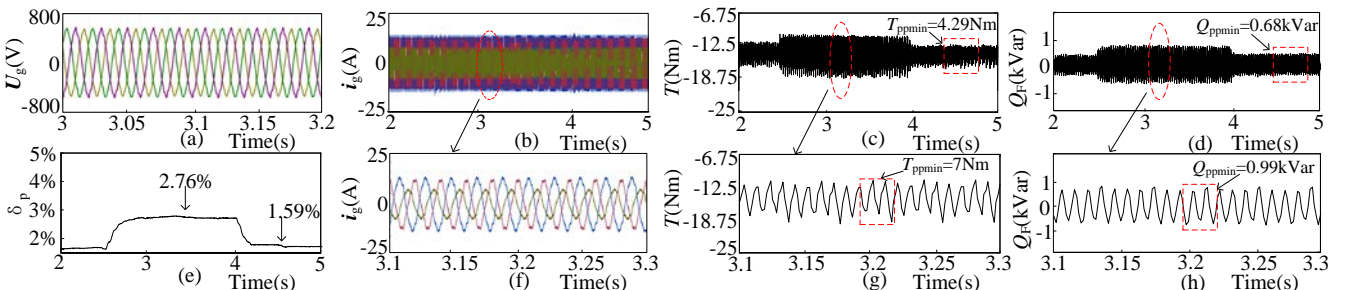


Fig. 11 Experimental results with proposed control strategy when average active power output of PMSG system steps with 3% VUF at terminal of PMSG system.

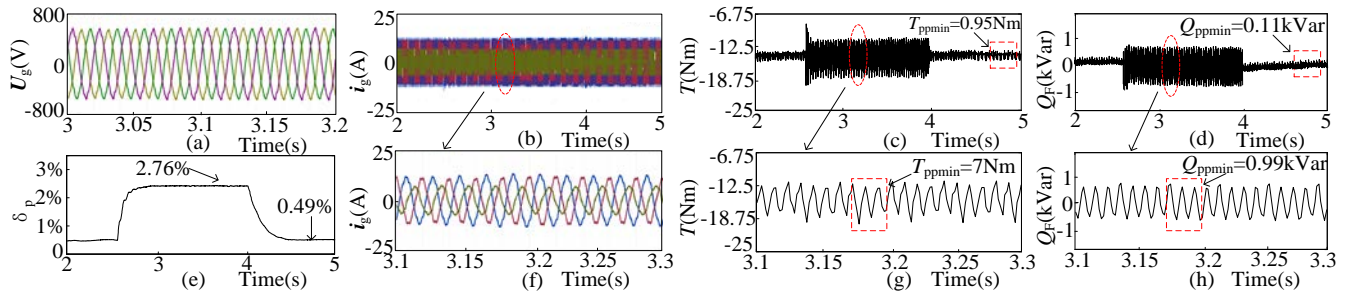


Fig. 12 Experimental results with proposed control strategy when VUF at terminal of PMSG system steps with 0.88 p.u. average active power output of PMSG system.

## VI. CONCLUSION

A hybrid wind farm with PMSG-based wind farm and FSIG-based wind farm under unbalanced grid voltage condition **has been** researched in this paper. The limit of negative-sequence current output of PMSG-based wind farm in a hybrid wind farm **has been** deduced, and the impacts of phase angle of the negative-sequence current on amplitude of negative-sequence voltage at PCC **have also been** analyzed. Furthermore, **the improved control strategy of injecting negative-sequence current by the designed negative-sequence voltage and current double close-loop control scheme in PMSG system has been developed for compensating the unbalanced voltage.** The theoretical analysis **indicates** that the amplitude of negative-sequence current of PMSG is limited by both active power output and DC link voltage of the PMSG system. In addition, the proposed **improved** control strategy can effectively mitigate VUF both at PCC and terminal of PMSG system to the optimal values **under any unbalanced grid voltage condition**, and the peak-to-peak double supply frequency pulsations in active and reactive power output of FSIG system can be effectively minimized. The theoretical analysis and proposed **improved** control strategy **have been** validated by experimental tests. The results show that the proposed **improved** control strategy can significantly improve the operation performance of FSIG system during network unbalance. It is noteworthy that, the theoretical analysis method and the **improved** control strategy presented in this paper can also be suitable for hybrid wind farm and other energy system based PWM converters, i.e., instance electrically excited synchronous generators, induction generators with full scale converters or photovoltaic power system, and the operation performance of entire hybrid energy system mentioned above will be significantly improved.

## APPENDIX A

### EXPERIMENT SYSTEM PARAMETERS

PMSG system parameters:

- 1) ratings:  $S_n=9$  kW,  $f_n=50$  Hz,  $U_n=380$  V (line to line rms),  $n_n=15$  r/s;  $V_{DC}=650$  V;
- 2) stator resistance: 0.09 p.u.;      3) inductance:  $L_d=0.78$  p.u.,  $L_q=1.07$  p.u.
- 4) reactor:  $L_g=0.1982$  p.u.;      5) DC link capacitor: 1100  $\mu$ F;
- 6) switching frequency: 12 kHz;

FSIG system parameters:

- 1) ratings:  $S_n=5.5$  kW,  $f_n=50$  Hz,  $U_n=380$  V (line to line rms),  $n_n=24$  r/s.
- 2) stator resistance: 0.234p.u.      3) stator leakage inductance: 0.056p.u.
- 4) rotor resistance: 0.374p.u.      5) rotor leakage inductance: 0.0187 p.u.
- 6) magnetizing inductance: 1.61p.u.

## REFERENCES

- [1] Shuhui Li, Timothy A. Haskew, Tichard P. Swatloski and William Gathings, "Optimal and direct-current vector control of direct-driven PMSG wind turbines," *IEEE Transactions on Power Electronics*, vol. 27, no. 5, pp. 2325-2337, May. 2012.
- [2] H. Li, and Z. Chen, "Overview of different wind generator systems and their comparisons," *IET Renewable Power Generation*, vol. 2, no. 2, pp. 123-138, 2008.
- [3] Akshaya Moharana, Rajiv K. Varma, and Ravi Seethapathy, "SSR alleviation by STATCOM in induction-generator-based wind farm connected to series compensated line," *IEEE Transactions on Sustainable Energy*, vol. 5, no. 3, pp. 947-957, Jul. 2014.
- [4] M. Firouzi, and G. B. Gharehpetian, "Improving fault ride-through capability of fixed-speed wind turbine by using bridge-type fault current limiter," *IEEE Transactions on Energy Conversion*, vol. 28, no. 2, pp. 361-369, Jun. 2013.
- [5] Ali Hooshyar, Maher Abdelkhalek Azzouz, and Ehab F. El-Saadany, "Distance protection of lines connected to induction generator-based wind farms during balanced faults," *IEEE Transactions on Sustainable Energy*, vol. 5, no. 4, pp. 1193-1203, Oct. 2014.
- [6] E. Muljadi, T. Batan, D. Yildirim, and C. P. Butterfield, "Understanding the unbalanced-voltage problem in wind turbine generation," in *Proc. IEEE Industry Applications Conference*, 1999, vol. 2, pp. 1359-1365.
- [7] T. Brekken and N. Mohan, "A novel doubly-fed induction wind generator control scheme for reactive power control and torque pulsation compensation under unbalanced grid voltage conditions," in *Proc. IEEE Power Electronics Specialist Conference*, 2003, vol. 2, pp. 760-764.
- [8] R. Piwko, N. Miller, J. Sanchez-Gasca, X. Yuan, R. Dai, and J. Lyons, "Integrating large wind farms into weak power grids with long transmission lines," in *Proc. IEEE Power Electronics and Motion Control Conference*, 2006, vol. 2, pp. 1-7.
- [9] S. Z. Chen, N. C. Cheung, K. C. Wong, and J. Wu, "Integral sliding-model direct torque control of doubly-fed induction generators under unbalanced grid voltage," *IEEE Transactions on Energy Conversion*, vol. 25, no. 2, pp. 356-368, Jun. 2010.
- [10] Mohamed El Moursi, Khaled Goweily, and Ebrahim A. Badran, "Enhanced fault ride through performance of self-excited induction generator-based wind park during unbalanced grid operation," *IET Power Electronics*, vol. 6, no. 8, pp. 1683-1695, 2013.
- [11] Christian Wessels, Nils Hoffmann, Marta Molinas, and Friedrich Wilhelm Fuchs, "StatCom control at wind farms with fixed-speed induction generators under asymmetrical grid faults," *IEEE Transactions on Industrial Electronics*, vol. 60, no. 7, pp. 2864-2873, Jul. 2013.
- [12] Jun Yao, Hui Li, Zhe Chen, Xianfeng Xia, Xiyin Chen, Qing Li, and Yong Liao, "Enhanced control of a DFIG-based wind-power generation system with series grid-side converter under unbalanced grid voltage conditions," *IEEE Transactions on Power Electronics*, vol. 28, no.7, pp. 3167-3181, Jul. 2013.
- [13] Andres E. Leon, Marcelo F. Farias, Pedro E. Battaio, Jorge A. Solsona, and María Inés Valla, "Control strategy of a DVR to improve stability in wind farms using squirrel-cage induction generators," *IEEE Transactions on Power Systems*, vol. 26, no. 3, pp. 1609-1617, Aug. 2011.
- [14] S. Zhang, K. Tseng, S. S. Choi, T. D. Nguyen, and D. Yao, "Advanced control of series voltage compensation to enhance wind turbine ride-through," *IEEE Transactions on Power Electronics*, vol. 27, no. 2, pp. 763-772, Feb.2012.

- [15] Yasser Abdel-Rady Ibrahim Mohamed and Ehab F. El-saadany, "A control scheme for PWM voltage-source distributed-generation inverters for fast load-voltage regulation and effective mitigation of unbalanced voltage disturbances," *IEEE Transactions on Industrial Electronics*, vol. 55, no.5, pp. 2072-2084, May. 2008.
- [16] Gustavo Azevedo, Pedro Rodriguez, Joan Rocabert, Marcelo Cavalcanti and Francisco Neves, "Voltage quality improvement of micro grids under islanding mode," in *Proc. IEEE Energy Conversion Congress and Exposition*, 2010, pp. 3169-3173.
- [17] Jinghang Lu, Farzam Nejabatkhah, Yunwei Li and Bin Wu, "DG control strategies for grid voltage unbalance compensation," in *Proc. IEEE Energy Conversion Congress and Exposition*, 2014, pp. 2932-2939.
- [18] Sarah Foster, Lie Xu, and Brendan Fox, "Coordinated reactive power control for facilitating fault ride through of doubly fed induction generator- and fixed speed induction generator-based wind farms," *IET Renewable Power Generation*, vol. 4, no. 2, pp. 128-138, 2010.
- [19] Andres E. Leon, Juan Manuel Mauricio, Antonio Gómez-Expósito, and Jorge Alberto Solsona, "An improved control strategy for hybrid wind farms," *IEEE Transactions on Sustainable Energy*, vol. 1, no. 3, pp. 131-141, Oct. 2010.
- [20] Yi Wang and Lie Xu, "Coordinated control of DFIG and FSI-based wind farms under unbalanced grid conditions," *IEEE Transactions on Power Delivery*, vol. 25, no.1, pp. 367-377, Jan. 2010.
- [21] A. F. Abdou, A. Abu-Siada, and H. R. Pota, "Damping of subsynchronous oscillations and improve transient stability for wind farms," in *Proc. IEEE Innovative Smart Grid Technologies Asia Conference*, 2011, pp. 1-6.
- [22] H. S. Song and K. Nam, "Dual current control scheme for PWM converter under unbalanced input voltage conditions," *IEEE Transactions on Industrial Electronics*, vol. 46, no. 5, pp. 953-959, Oct. 1999.
- [23] Voltage characteristics of electricity supplied by public distribution systems, EN 50160, 1999.
- [24] Technical rule for connecting wind farm to power system, GB/T 19963-2011, 2012.
- [25] Shao Zhang, King-Jet Tseng, D. Mahinda Vilathgamuwa, Trong Duy Nguyen, and Xiao-Yu Wang, "Design of a robust grid interface system for PMSG-based wind turbine generators," *IEEE Transactions on Industrial Electronics*, vol. 58, no. 1, pp. 316-328, Jan. 2011.
- [26] Hua Geng, Dewei Xu, Bin Wu, and Geng Yang, "Active damping for PMSG-based WECS with DC-link current estimation," *IEEE Transactions on Industrial Electronics*, vol. 58, no. 4, pp. 1110-1119, Apr. 2011.
- [27] Hamid Shariatpanah, Roohollah Fadaeinedjad, and Masood Rashidinejad, "A new model for PMSG-based wind turbine with yaw control," *IEEE Transactions on Energy Conversion*, vol. 28, no. 4, pp. 929-937, Dec. 2013.